*Research article*

# Transient H₂O₂ Induction by ClO₂ Fumigation Alters Prx-Trx System and Causes MAPK Accumulation Attenuating Browning in Harvested Longan Fruit

**Athiwat Chumyam[1] and Kobkiat Saengnil[1, 2, 3, *]**

1 Department of Biology, Faculty of Science, Chiang Mai University, Chiang Mai 50200, Thailand
2 Research Center in Bioresources for Agriculture, Industry and Medicine, Faculty of Science, Chiang Mai University, Chiang Mai 50200, Thailand
3 Postharvest Technology Innovation Center, Ministry of Higher Education, Science, Research and Innovation, Bangkok 10400, Thailand

**Abstract** Peroxiredoxin-thioredoxin (Prx-Trx) system plays a critical role in both redox sensing and controlling of signal transduction pathways. This study aimed to demonstrate the effects of chlorine dioxide (ClO₂) fumigation on the alteration of redox status of peroxiredoxin (Prx) and thioredoxin (Trx) in hydrogen peroxide (H₂O₂) sensing and the activation of mitogen-activated protein kinase (MAPK) involved in signal transduction and pericarp browning of longan fruit. After fresh longan fruit were fumigated with 10 mg L$^{-1}$ ClO₂ for 10 min, a transient peak of H₂O₂ was found at 6 h. It also led to strong accumulation of mitogen-activated protein kinases 3 and 6 (MPK3 and MPK6) that persisted up to 3-5 d after fumigation. Furthermore, the oxidation state as well as reductase activities of both Prx and Trx increased concurrently, reaching their peaks at 12-24 h after fumigation. Both redox state and redox potential of nicotinamide adenine dinucleotide phosphate were significantly affected throughout the time of storage (7 d). The altered Prx and Trx redox state and accumulation of MPK3 and MPK6 were closely associated with the reduction in excessive H₂O₂ accumulation and pericarp browning after 24 h of fumigation. These findings indicated that ClO₂ may trigger the H₂O₂-induced Prx/Trx redox cycling and MAPK activity, resulting in the reduction of pericarp browning of longan fruit during storage.

**Keywords:** Chlorine dioxide, *Dimocarpus longan* Lour. , MAPK, Prx-Trx system, Redox potential, Signal transduction

# INTRODUCTION

Reactive oxygen species (ROS), such as hydrogen peroxide ($H_2O_2$), can be beneficial or detrimental to cell physiology (Veal et al., 2007). Excessive accumulation of $H_2O_2$ leads to the production of various free radicals which damage cell constituents, disturb cell functions and, ultimately, lead to cell death (Sharma et al., 2012; Liu and He, 2017). On the other hand, $H_2O_2$ is necessary for some physiological processes. For example, it interacts with thiol-containing proteins and activates different signaling pathways regulating gene expression and cell-cycle processes (Ślesak et al., 2007; Veal et al., 2007). Peroxiredoxin (Prx) is the first target in the $H_2O_2$-induced signaling pathway. The oxidized Prxs transfer signal through either thiol-disulfide redox reaction or non-redox protein-protein interaction (Randall et al., 2013).

The peroxiredoxin-thioredoxin (Prx-Trx) system consists of thioredoxin (Trx), Prx and thioredoxin reductase (TrxR). The system plays a critical role in the defense against oxidative stress by removing harmful $H_2O_2$ using reduced nicotinamide adenine dinucleotide phosphate (NADPH) as a reducing agent (Dietz et al., 2006; Pannala and Dash, 2015). Lesser activities of Prx and TrxR and the lower ratio of NADPH/oxidized nicotinamide adenine dinucleotide phosphate (NADP) reduce the capacity of the Prx-Trx system to control cellular concentration of $H_2O_2$, leading to oxidative damage and cell senescence (Rhee et al., 2012; Sevilla et al., 2015; Chumyam et al., 2019).

Recent studies have demonstrated that plant defense system could be activated through the alteration of ratio of oxidized Prx ($Prx_{ox}$) to reduced Prx ($Prx_{red}$) ($Prx_{ox}/Prx_{red}$ ratio) and the ratio of oxidized Trx ($Trx_{ox}$) to reduced Trx ($Trx_{red}$) ($Trx_{ox}/Trx_{red}$ ratio) during stresses or chemical treatments. It was found that the increases in $Prx_{ox}/Prx_{red}$ and $Trx_{ox}/Trx_{red}$ ratios activated defense system in barley seedlings under salt stress and $H_2O_2$ treatment (König et al., 2002) and in Chinese cabbage under heat shock and oxidative stress (Kim et al., 2009)

In plants, Trx and Prx are involved in the control of dithiol-disulfide exchanges of target proteins during development and stress adaptation (Sevilla et al., 2015). Prx facilitates $H_2O_2$ signaling by regulating cellular $H_2O_2$ level, therefore, mediating interaction between $H_2O_2$ and its target signaling protein. Moreover, the target signaling proteins are also controlled by the redox state of Prx and Trx. A significant increase in $Prx_{ox}/Prx_{red}$ and $Trx_{ox}/Trx_{red}$ ratios signals protein oxidation in the target signaling protein (Brown et al., 2013; Netto and Antunes, 2016). The oxidized signaling protein activates signal transduction effectors including kinases, phosphatases and transcription factors (Cross and Templeton, 2006).

Among the target signaling proteins, the mitogen-activated protein kinases (MAPKs) play an important role in protein phosphorylation of signal transduction in plants (Ye et al., 2015; Liu and He, 2017). Mitogen-activated protein kinases 3 and 6 (MPK3 and MPK6) have been identified as the main isoform of plant MAPK. It is highly induced under abiotic stress and response through $H_2O_2$ signaling (Ye et al., 2015; Liu and He, 2017). In *Arabidopsis thaliana*, AtMPK3 and AtMPK6 are activated by various concentrations of $H_2O_2$ resulting in tolerance to freezing, heat and salt stresses (Kovtun et al., 2000). In addition, jasmonic acid also induces $H_2O_2$ signaling and activates MAPK/extracellular signal-regulated kinase, resulting in upregulating the redox states of ascorbate and glutathione and increasing antioxidant enzyme activities in wheat (Dai et al., 2015).

Longan (*Dimocarpus longan* Lour. cv. Daw), an important economic fruit in Thailand, undergoes rapid pericarp browning after a few days at room temperature, resulting in short storage life and reduction in market value (Saengnil et al., 2014). However, applications of gaseous chlorine dioxide ($ClO_2$) at 10 mg $L^{-1}$ for 10 min to longan fruit before storage at 25 °C significantly reduce pericarp browning by reducing the oxidation of phenolic compound, maintaining higher fruit quality longer (Saengnil et al., 2014). One mechanism by which $ClO_2$ reduces longan pericarp browning is due to the enhancement of antioxidant defense system (Chomkitichai et al., 2014a, 2014b). Interestingly, a relationship between $ClO_2$-activated reduction of pericarp browning and $H_2O_2$ signaling has been reported recently (Joradol et al., 2019).

Several lines of evidence have suggested that $H_2O_2$ signaling, Prx-Trx redox system and MAPK cascades work in concert in stress responses. It is plausible that the same scenario exists in harvested longan and is enhanced by $ClO_2$ fumigation. Therefore, the objective of this research was to investigate the effects of $ClO_2$ on $H_2O_2$ production, redox status in Prx-Trx system, MPK3 and MPK6 activation and pericarp browning of 'Daw' longan fruit during storage.

# MATERIALS AND METHODS

## Plant materials and $ClO_2$ treatments

Longan fruit cv. Daw at the harvesting stage (180 d after full bloom, 15-16% total soluble solid) were obtained from a commercial orchard in Lamphun province, Thailand and transported to the Postharvest Physiology and Technology Research Laboratory at Chiang Mai University under 25 °C within 2 h. Fruit were selected for uniformity in shape, color, size and lack of defects and divided into 6 groups of 330 fruit each. $ClO_2$ gas was prepared according to Saengnil et al. (2014). The most effective concentration for reducing pericarp browning and maintaining fruit quality of longan was 10 mg $L^{-1}$ for 10 min (Saengnil et al., 2014). A 10 min fumigation with 0 and 10 mg $L^{-1}$ $ClO_2$ was done in a chamber separately in triplicate. After fumigation, the chamber was ventilated for 30 min to remove any residual $ClO_2$. The fumigated fruit in each group were placed in a commercial cardboard box (25 cm (L) × 17 cm (W) × 9 cm (H)), 30 fruit per box. All the boxes were stored in a storage room at 25 ± 1 °C with a relative humidity of 82 ± 5% for 7 d. Thirty fruit from each treatment were taken at 0, 6, 12 and 24 h and, thereafter, once a day for 6 d to determine the biochemical changes.

## Determination of $H_2O_2$ content

$H_2O_2$ content was determined according to the method of Velikova et al. (2000) with slight modifications. Pericarp of 30 fruit in each treatment was cut into small pieces and thoroughly mixed. One gram of the pericarp was homogenized in 10 mL of 1% trichloroacetic acid (TCA) at 4 °C for 1 min. The homogenate was centrifuged at 20,000 × g and 4 °C for 20 min. The supernatant (0.5 mL) was added to 1.5 mL of 10 mM potassium phosphate buffer (K-P buffer) (pH 7.0) and 1 mL of 1 M potassium iodide. The absorbance of the mixture was measured at 390 nm (distilled water was used as blank). The standard curve was constructed using $H_2O_2$, which was expressed as mmol $kg^{-1}$.

## Redox Assay of Prx and Trx

Protein extraction and western blot analysis were determined according to the methods of Go and Jones (2009) and Muniyappa et al. (2009) with some modifications.

For Prx extraction, 2 g of the pericarp (from 30 fruit) were sampled and ground in liquid nitrogen. The powder was then homogenized in 5 mL of 50 mM tris hydrochloride (Tris-HCl) buffer (pH 8.0) containing 1 mM ethylenediamine tetraacetic acid (EDTA), 20% sucrose, 0.75% potassium chloride, 2% polyvinylpolypyrrolidone (PVPP) and protease inhibitor cocktail at 4 °C for 1 min. The homogenate was centrifuged at 16,000 × g and 4 °C for 20 min. The supernatant was transferred to fresh tubes and extracted with 3 mL of buffer saturated phenol. The mixture was then centrifuged at 16,000 × g and 4 °C for 20 min and the top layer (phenol phase) was collected. The protein was precipitated with 9 mL of 0.1 M ammonium acetate in methanol at -20 °C overnight and centrifuged at 16,000 × g and 4 °C for 10 min and the supernatant was removed. The pellet was washed with precipitation buffer twice and recovered by centrifugation at 10,000 × g and 4 °C for 5 min. The final precipitate was dissolved in 100 μL of 100 mM Tris-HCl buffer (pH 6.8). Protein content was determined by the Lowry method (Lowry et al., 1951).

For Trx extraction, 2 g of pericarp (from 30 fruit) were sampled and ground in liquid nitrogen. The powder was then homogenized in 5 mL of 50 mM Tris-HCl buffer (pH 8.2) containing 1 mM EDTA, 30 mM iodoacetic acid (IAA) and protease inhibitor cocktail at 4 °C for 1 min. After homogenization, 5 μL of 10% Triton X-100 was added to the tubes, and the tubes were incubated at 37 °C in the dark for 1 h, then centrifuged

at 10,000 × g and 4 °C for 10 min and transferred to fresh tubes. To wash away excess IAA, the protein was precipitated with 15 mL of ice-cold acetone: 1 M hydrochloric acid (HCl) (98:2, v:v) and centrifuged at 16,000 × g and 4 °C for 10 min and the supernatant was removed. This washing procedure was repeated twice. The final precipitate was dissolved in 100 µL of 50 mM Tris-HCl buffer (pH 8.2) containing 1 mM EDTA. Protein content was determined by the Lowry method.

Twenty micrograms of protein was separated on 15% non-reducing polyacrylamide gel electrophoresis (PAGE) (for Prx) or 15% native PAGE (for Trx). Following electrophoresis, proteins were transferred to nitrocellulose membrane using a semi-dry BioRad system. The membrane was first blocked for 30 min with 1% bovine serum albumin (BSA) in Tris-buffered saline containing Tween 20 (TBST) before incubation with primary antibody, polyclonal rabbit IgG anti-Trx (Aviva, Aviva Systems Biology Corporation, San Diego, CA, USA, Catalog #  ARP72618_P050) (1:1000 dilution) or polyclonal rabbit IgG anti-Prx (BosterBio, Boster Biological Technology, Pleasanton, CA, USA, Catalog #  PA1834) (1:1,000 dilution) in a solution of 1% BSA in TBST at 37 °C for 1 h followed by 5 °C overnight. After washing with TBST, the membrane was incubated again with the secondary antibody, goat anti-rabbit IgG alkaline phosphatase conjugate (Jackson Immuno, Jackson Immuno Research Inc., West Grove, PA, USA, Catalog # 111-055-003) (1:5000 dilution) in a solution of 1% BSA in TBST at 37 °C for 1.5 h. The membrane was then washed with TBST. Nitro blue tetrazolium/ 5-bromo-4-chloro-3-indolyl phosphate (NBT/BCIP) substrate was used in the detection of secondary antibody. Redox state of Prx and Trx was quantified from band intensities between oxidized and reduced forms using ImageJ (LOCI, USA) and expressed as oxidized/reduced form ratios.

## Assay of MPK3 and MPK6 accumulation

Protein extraction and western blot analysis were determined according to the method of Frey et al. (2014) with some modifications. Approximately 100 mg of frozen longan pericarp (from 30 fruit) were ground in liquid nitrogen and resuspended in 200 µL of extraction buffer containing 50 mM Tris-HCl buffer (pH 7.5), 150 mM sodium chloride, 5 mM EDTA, 0.1 mM dithiothreitol and protease inhibitor cocktail. The suspension was centrifuged at 20,000 × g and 4 °C for 15 min and the supernatant was collected. Protein content was determined by the Lowry method. Protein samples (20 µg) were separated on 10% sodium dodecyl sulfate polyacrylamide gel electrophoresis and transferred onto nitrocellulose membrane. The membrane was first blocked for 30 min with 1% BSA in TBST buffer and the incubation was then continued with primary antibody, polyclonal rabbit IgG anti-MPK3 or MPK6 (BosterBio, Boster Biological Technology, Pleasanton, CA, USA, Catalog # A04510 and A30170) (1:1000 dilution) in a solution of 1% BSA in TBST at 37 °C for 1 h followed by 5 °C overnight. After washing, the membrane was incubated again with the secondary antibody, goat anti-rabbit IgG alkaline phosphatase conjugate (Jackson Immuno, Jackson Immuno Research Inc., West Grove, PA, USA, Catalog # 111-055-003) (1:5000 dilution) in a solution of 1% BSA in TBST at 37 °C for 1.5 h. Following this step, the membrane was washed and the secondary antibody was detected using NBT/BCIP substrate. Polyclonal rabbit IgG anti-GAPDH (Boster Biological Technology, Pleasanton CA, USA, Catalog # A00227-1) was used to detect a reference protein.

## Determination of Prx and TrxR activities

Prx and TrxR activities were determined according to the methods of Arnér et al. (1999) and Pascual et al. (2011) with slight modifications. One gram of pericarp (from 30 fruit) was sampled and homogenized in 10 mL of 25 mM K-P buffer (pH 7.0) containing 2.5 mM EDTA at 4 °C for 1 min. The homogenate was centrifuged at 15,000 × g and 4 °C for 15 min and the supernatant was collected. Prx activity was assayed in 1.8 mL of a reaction mixture containing 100 mM K-P buffer (pH 7.0), 10 mM EDTA, 0.24 mM NADPH, 0.5 mM $H_2O_2$ and 0.2 mL of the supernatant. The subsequent decrease in NADPH was measured at 340 nm (molar extinction coefficient = 6.2 mM$^{-1}$ cm$^{-1}$). TrxR activity was assayed in 0.9 mL of 100 mM K-P buffer (pH 7.0) containing 10 mM EDTA, 0.24 mM NADPH, 0.07 mL of the supernatant and 0.03 mL of 0.1 mM 5,5′-Dithiobis-(2-nitrobenzoic acid) (DTNB) in dimethyl sulfoxide. The changes in DTNB was observed at

412 nm (molar extinction coefficient = 13.6 $mM^{-1}$ $cm^{-1}$). The Prx and TrxR activities were expressed as mmol $min^{-1}$ $kg^{-1}$ protein.

## Determination of NADP and NADPH contents

NADP and NADPH contents were assayed by the procedure of Brugidou et al. (1991) with some modifications. One gram of the pericarp (from 30 fruit) was sampled and homogenized in 10 mL of 0.5 M perchloric acid in 10% methanol for NADP extraction, or 0.5 M sodium hydroxide in 10% methanol for NADPH extraction at 4 °C for 1 min. The homogenate was then centrifuged at 5,000 × g and 4 °C for 15 min. The supernatant was adjusted to either pH 5.0 with 6 M potassium hydroxide for the NADP extraction or pH 8.0 with 1 M HCl for the NADPH extraction and filtered through a 0.45 µm filter (MS® Nylon Syringe Filter, Membrane Solution, Kent, WA, USA). Twenty microliter of the supernatant was separated by high performance liquid chromatography (HPLC) system using a reserved phase Eclipse XDB-C18 column (Agilent, Agilent Corporation, Santa Clara, CA, USA) with 0.1 M K-P buffer (pH 6.0) and 0.1 M K-P buffer in 20% methanol (pH 6.0) as mobile phases and measured at 254 nm. HPLC separation was achieved using continuous gradient elution at a flow rate of 1.3 mL $min^{-1}$. NADP and NADPH contents were determined using the external standard method. The redox status of NADP was expressed as the ratio of NADPH to NADP while the NADP redox potential was calculated using Nernst equation: *E = $E_0$ – RT/nF In(NADPH/NADP)* (Schafer and Buettner, 2001).[10]

## Determination of polyphenol oxidase (PPO) activity

The PPO activity was assayed according to the method of Saengnil et al. (2014) with some modifications. Longan pericarp (1 g) was sliced and homogenized in 10 mL of 0.05 M K-P buffer (pH 6.2) containing 2% PVPP at 4 °C for 1 min. The homogenate was centrifuged at 20,000 × g and 4 °C for 5 min. The supernatant was collected as a crude enzyme extract to determine PPO activity. PPO activity was assayed in 1.5 mL of reaction mixture containing 0.05 M K-P buffer (pH 7.5), 0.2 M catechol and 0.5 mL of crude enzyme. The mixture was incubated for 5 min at room temperature. The absorbance was measured at 420 nm. The unit of enzyme activity was defined as the amount of enzyme that caused a change of 0.01 in absorbance per min and expressed as kU $kg^{-1}$ protein.

## Determination of total phenolic (TP) content

TP content was determined according to the method of Saengnil et al. (2014) with some modifications. Longan pericarp (1 g) was sliced and homogenized in 10 mL of 80% ethanol at 4 °C for 1 min. The homogenate was centrifuged at 16,000 × g and 4 °C for 20 min. Then 0.4 mL of the supernatant was mixed with 2 mL of 10% Folin-Ciocalteu's phenol reagent for 8 min and 1.6 mL of 7.5% sodium carbonate was added. The mixture was kept at room temperature for 2 h. The absorbance was measured at 765 nm. TP content was determined from the linear equation of a standard curve prepared with gallic acid and expressed as g $kg^{-1}$.

## Evaluation of pericarp browning

The browning of longan pericarp was assessed using two different methods. Firstly, pericarp browning was estimated using the browning index (BI) (Jiang and Li, 2001). Browning was estimated visually by measuring the extent of the total brown area on each fruit surface (for 30 fruit) using the following scale: 1 = no browning (excellent quality), 2 = 1-10% browning, 3 = 11-25% browning, 4 = 25-50% browning and 5 = >50% browning (poor quality). BI was calculated using the following formula: *BI = {∑ (browning scale × number of fruit in each scale)} / total number of fruit*. Fruit having BI above 3.0 were considered as unacceptable for market quality. Secondly, the method of browning assessment was modified from Supapvanich et al. (2011) where 0.5 g of freeze dried longan pericarp was homogenized in 20 mL of 65% ethanol for 1 min. The mixture was left at 27 °C for 30 min. Then, the extract was filtered with Whatman® No.1 filter paper. Absorbance of the extract was measured at 420 nm.

### Statistical analysis

All statistical analyses were performed using Statistical Packages for the Social Science (SPSS, SPSS: An IBM Company, Armonk, NY, USA) version 22.0. Data were tested by t-test and Mann-Whitney test at a significant level of 0.05. Experiments were repeated twice and similar results were obtained. The results of one representative experiment were shown and the data were presented as mean ± standard deviation (SD).

## RESULTS

### Effects of $ClO_2$ on $H_2O_2$ content

$ClO_2$ treatment significantly caused rapid and transient increase in $H_2O_2$ level in longan pericarp. The level reached its peak soon after 6 h of fumigation and decreased to the basal level as fast. At the highest peak, the $H_2O_2$ level was 2.2 folds higher than that of the control which increased slightly during the same period (Figure 1). The $H_2O_2$ level of the control started to increase after 12 h of storage while that of the $ClO_2$ treated fruit did not rise again until 48 h later. In addition, the $H_2O_2$ level did not rise as fast and remained significantly lower (33.3-55.5%) than that of the control until the end of storage (Figure 1).
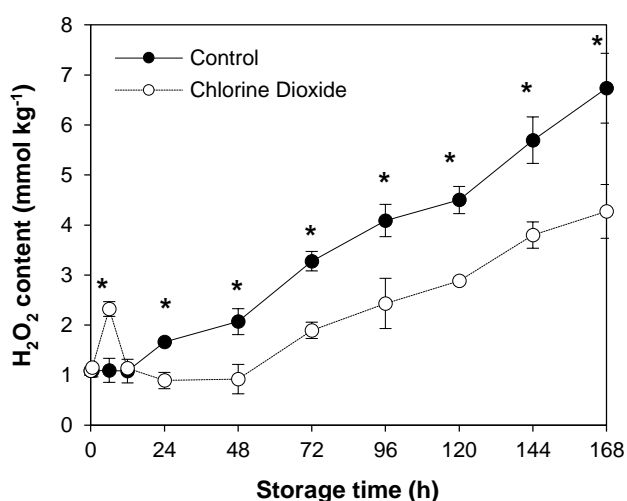


**Figure 1. Effects of $ClO_2$ on $H_2O_2$ content of longan pericarp during storage.** The $H_2O_2$ content was extracted from pericarp and measured by spectrometry method. Data are shown as the mean ± SD ($n$ = 3). Bars with * indicate significant difference between $ClO_2$ treated and control fruit using t-test at $P < 0.05$.

### Effects of $ClO_2$ on Prx and Trx redox state

$ClO_2$ fumigation caused both Prx and Trx redox state to change significantly during the first 2 d after fumigation (Figure 2). Compared to that of the untreated control, $Prx_{ox}/Prx_{red}$ ratio of the fumigated group rose immediately and reached the highest level, 4 times higher, at 24 h before dropping significantly to a lower level on day 2 (Figure 2a). Similarly, $Trx_{ox}/Trx_{red}$ ratio of the treated fruit suddenly increased after fumigation, reaching the highest level at 24 h, 2 folds greater and dropped precipitously afterward (Figure 2b). $Prx_{ox}/Prx_{red}$ and $Trx_{ox}/Trx_{red}$ ratios of both groups increased at a similar rate starting from day 2. However, those of the fumigated fruit remained significantly lower at 16.2-58.2% and 25-46.2%, respectively, than that of the control until the end of storage (Figure 2).
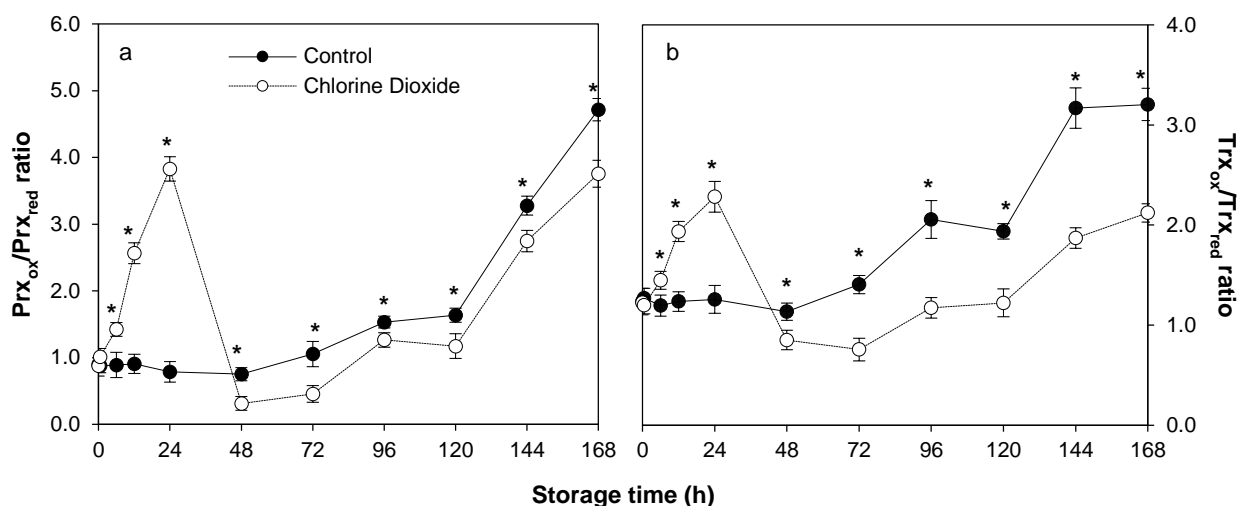
**Figure 2. Effects of $ClO_2$ on Prx (a) and Trx (b) redox state of longan pericarp during storage.** Prx and Trx redox state were assayed by comparing the band intensities between oxidized and reduced forms of Prx or Trx proteins using western blot analysis with Prx and Trx specific antibodies. Data are shown as the mean ± SD ($n$ = 3). Bars with * indicate significant difference between $ClO_2$ treated and control fruit using t-test at $P < 0.05$.

## Effects of $ClO_2$ on Prx and TrxR enzymatic activities

The activities of both enzymes in the fumigated samples were significantly enhanced during the first 12-24 h (Figure 3). It seemed to be a two-step increase in the Prx activity, the rapid rise occurred immediately lasting about 6 h, followed by a more modest increase until reaching its peak, 61% higher than that of the untreated control, at 24 h after fumigation. In comparison, Prx activity of the control rose only slightly during the first 6 h. The activity of the enzyme of both fumigated and control groups similarly and gradually declined for the next 3 to 4 d. However, Prx activity of the former remained significantly higher, showing 6-107% higher for the first 4 d (Figure 3a).

Unlike Prx, the activity of TrxR in both control and $ClO_2$-treated fruit increased immediately but at a different rate. The former rose more gradually and reached the highest level at 24 h, while the latter rapidly surged reaching its peak at 12 h (70% higher than the untreated control) and decreased gradually thereafter. $ClO_2$ fumigation resulted in significantly higher TrxR activity at 32.4-96.3% for the first 4 d (Figure 3b).
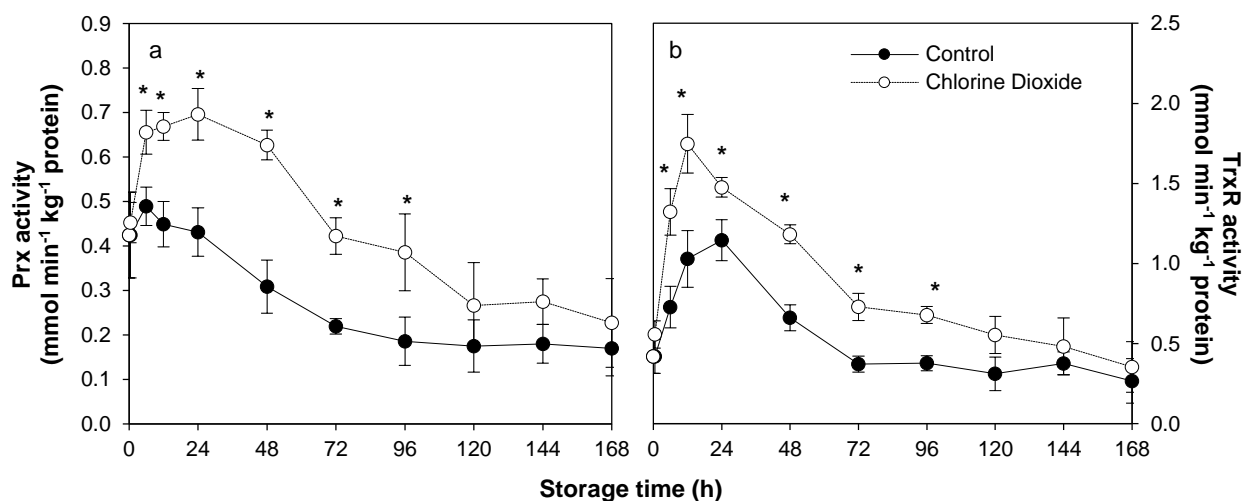


**Figure 3. Effects of $ClO_2$ on Prx (a) and TrxR (b) activities of longan pericarp during storage.** The enzyme activities was measured by spectrometry method with specific substrate. Data are shown as the mean ± SD (n = 3). Bars with * indicate significant difference between $ClO_2$ treated and control fruit using t-test at $P < 0.05$.

## Effects of $ClO_2$ on MPK3 and MPK6 accumulation

$ClO_2$ fumigation caused accumulation of MPK3 and MPK6 (Figure 4). The kinases could be detected immediately after fumigation and became most prominent at 12 h. It should be noted that the intensity of the band corresponding to MPK6 was much higher than that of MPK3. Moreover, MPK6 could be detected up to day 5 while the other was barely detectable on day 4 (Figure 4).



**Figure 4. Effects of $ClO_2$ on MPK3 and MPK6 accumulation in longan pericarp during storage.** Western blot analysis of MPK3 and MPK6 protein in longan pericarp between $ClO_2$ treatment and control group. MPK3 and MPK6 protein amounts were detected with specific antibody. The protein band corresponding to the GAPDH showed equal loading. BF = before fumigation. AF = after fumigation.

## Effects of $ClO_2$ on NADP redox state and redox potential

The changes in the NADP redox state (as described by NADPH/NADP ratio) of $ClO_2$-fumigated fruit were dramatic. The ratio rose sharply immediately after fumigation reaching maximum at 6 h (42% higher than the untreated control) before declining slowly thereafter. In contrast, the redox state of the control fruit started to decrease slowly from the start. The rate of the decrease was similar in both groups but the ratio of $ClO_2$-fumigated fruit was 22.4-44.6% significantly higher over the storage time (Figure 5a).

Using Nernst equation, NADP redox potential was calculated and compared between the $ClO_2$-fumigated and control fruit. It was found that there were small but significant differences in the redox potential between the two groups. The differences were between 0.8-1.5% throughout storage. After $ClO_2$ fumigation, NADP redox potential decreased immediately to the lowest level at 6 h (1.41% higher than the untreated control) before rising thereafter (Figure 5b). In contrast, the redox potential of the control fruit started to increase slowly from the start. The rate of the increase was similar in both groups but the redox potential of $ClO_2$-fumigated fruit was significantly lower over the storage time (Figure 5b).
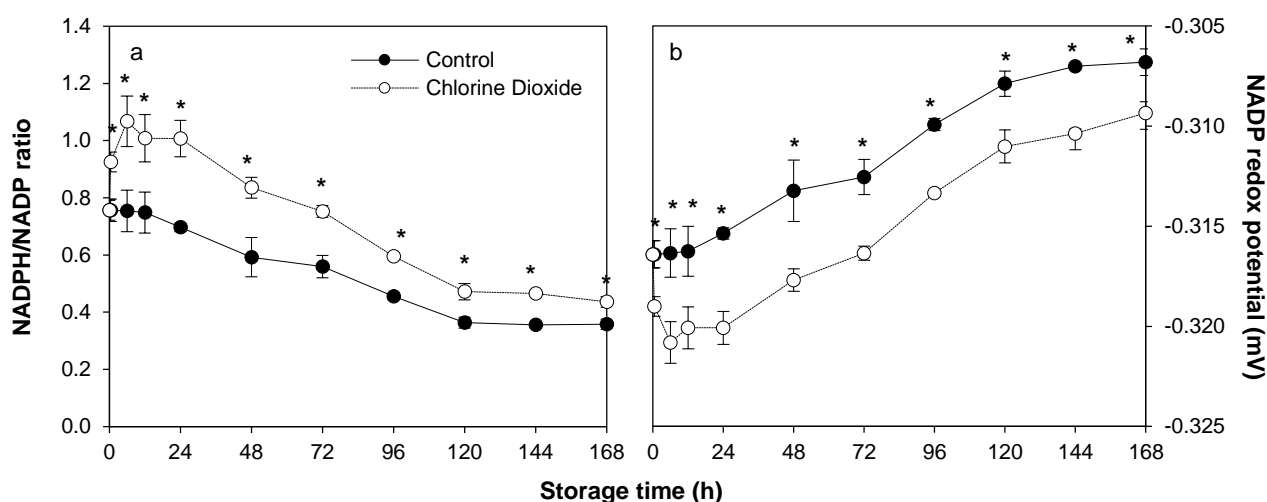
**Figure 5. Effects of ClO₂ on NADPH/NADP ratio (a) and NADP redox potential (b) of longan pericarp during storage.** NADPH and NADP was measured using HPLC method and expressed as the ratio between NADPH to NADP content. The NADP redox potential was calculated using Nernst equation. Data are shown as the mean ± SD (*n* = 3). Bars with * indicate significant difference between ClO₂ treated and control fruit using t-test at *P* <0.05.

## Effects of ClO₂ on PPO activity and TP content

PPO activity in the control fruit rapidly increased and reached its peak on day 2 and then decreased gradually during storage (Figure 6a). Change in PPO activity in the pericarp of the fruit fumigated with ClO₂ showed a similar pattern to the control fruit but the activity was lower than the control. PPO activity in the ClO₂ fumigated fruit was significantly lower than the control by 4.7-15.8% during storage (Figure 6a).

TP content in the control fruit continuously decreased throughout the storage time (Figure 6b). However, ClO₂ fumigation delayed the decrease in TP content during storage. The fruit fumigated with ClO₂ showed a similar pattern to the control fruit but had significantly higher TP content. TP content in the fumigated fruit was 1.3-25.0% higher than the control fruit over storage time (Figure 6b).
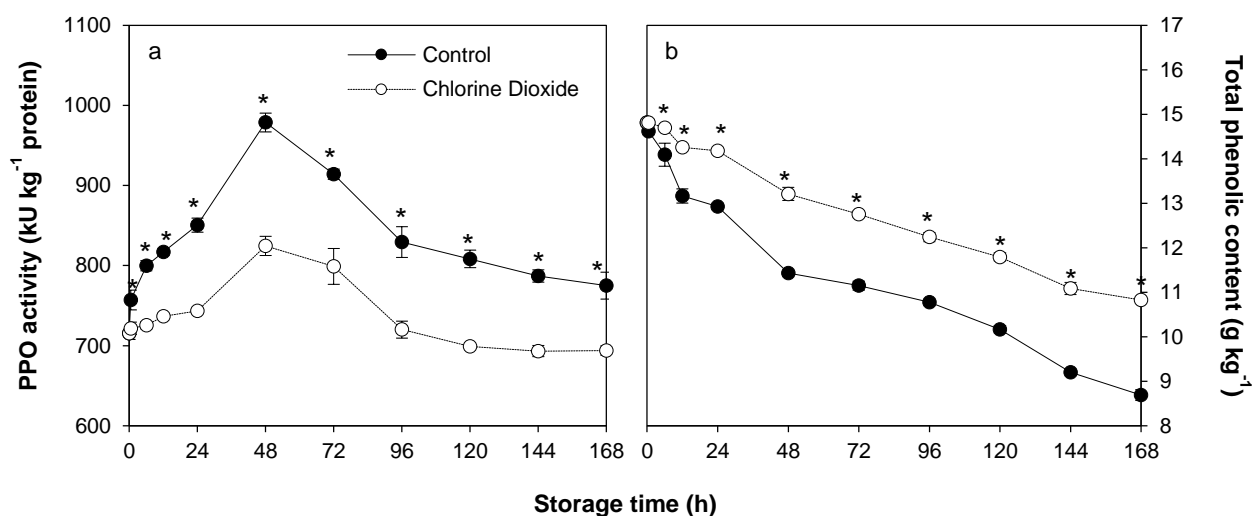


**Figure 6. Effects of ClO₂ on PPO activity (a) and TP content (b) of longan pericarp during storage.** PPO activity and TP content was measured by spectrometry method. Data are shown as the mean ± SD (*n* = 3). Bars with * indicate significant difference between ClO₂ treated and control fruit using t-test at *P* <0.05.

### Effects of $ClO_2$ on browning

The BI of the control fruit increased rapidly with increasing storage time and became unacceptable after 3 d of storage. $ClO_2$ fumigation significantly reduced BI and, consequently, extended the shelf life further for another 3 d (Figure 7a). Browning assessed by measuring the optical density at 420 nm in both $ClO_2$-fumigated and the control fruit increased continuously with storage time. There was a 6 h delay in the fumigated group before the increase. In addition, $OD_{420}$ was significantly lower than that of the control group by 3.33-7.27% during 12 h to 6 d of storage (Figure 7b).
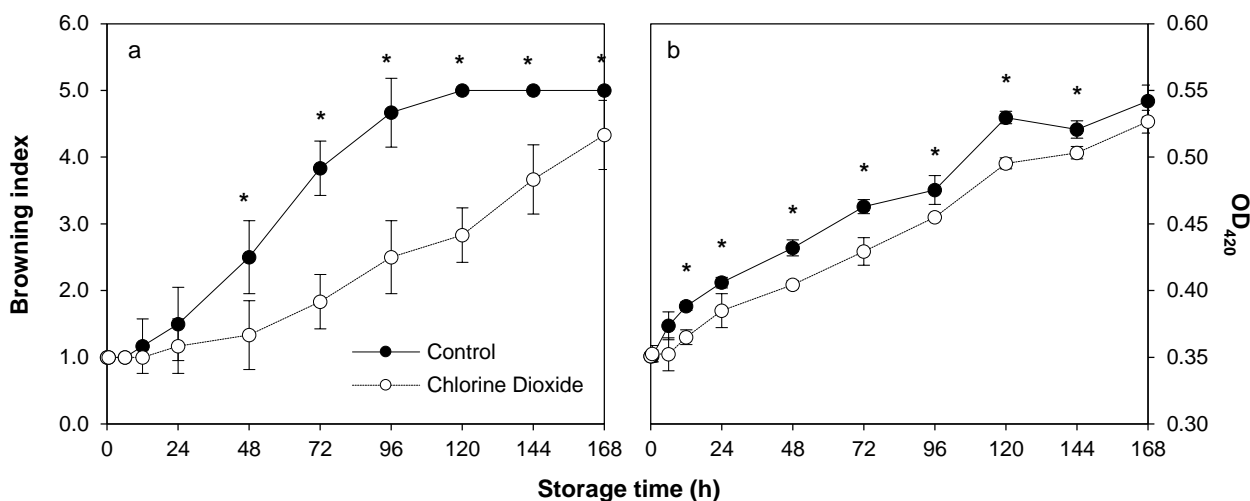


**Figure 7. Changes of longan BI (a) and browning as determined using optical density at 420 nm (b) between $ClO_2$ treated and control fruit during storage**. BI was assayed by scoring the intensity of brow area on fruit surface whereas the $OD_{420}$ was measured from pericarp extract using spectrometry method. Data are shown as the mean ± SD ($n$ = 3). Bars with * indicate significant difference between $ClO_2$ treated and control fruit using Mann-Whitney test (BI) and t-test ($OD_{420}$) at $P$ <0.05.

## DISCUSSION

Plants rapidly produce $H_2O_2$ during exposure to a variety of chemicals or sub-optimal physical and biological conditions (Veal et al., 2007). The results clearly showed that transient $H_2O_2$ generation was induced in $ClO_2$ fumigated fruit during the first 6 h of storage (Figure 1). Previous studies have demonstrated similar rapid production of $H_2O_2$ in wheat leaves treated with jasmonic acid (Dai et al., 2015), mustard seedlings treated with salicylic acid (SA) (Dat et al., 1998), citrus fruit treated with SA (Zhu et al., 2016) and longan fruit fumigated with $ClO_2$ (Joradol et al., 2019). Plant cells produce $H_2O_2$ primarily through the activity of NADPH oxidase (NOX) to mediate instant systemic signaling when facing abiotic stresses (Rhee et al., 2003). The enzyme reduces oxygen forming superoxide anion radical which is converted to $H_2O_2$ by superoxide dismutase (SOD) (Joradol et al., 2019).

The rapid production and degradation of $H_2O_2$ is like other specific signaling molecules. It is possible that $ClO_2$ might activate the gene expression and the enzyme activity of NOX and SOD, resulting in $H_2O_2$ production which activates the antioxidant defense mechanism. Oxidative membrane damage is postponed or reduced leading to the reduction in phenolic oxidation by PPO and POD (Chomkitichai, 2014). In this study, it was also found that $ClO_2$ reduced the activity of PPO and maintained higher TP content during storage of longan fruit (Figure 6). Moreover, the pericarp browning was also reduced (Figure 7). This indicates that reduction of longan pericarp browning through

the reduction of phenolic oxidation by $ClO_2$ might be due to the induction of transient $H_2O_2$.

Prx and Trx redox state has also been reported recently to play an important role in the regulation of $H_2O_2$ sensing and antioxidant defense system (Dietz et al., 2006; Pannala and Dash, 2015; Netto and Antunes, 2016). It was found that $Prx_{ox}/Prx_{red}$ and $Trx_{ox}/Trx_{red}$ ratios increased in stepwise fashion. The first slower phase occurs during the first 6 h. The following second phase was faster and lasted until 24 h after fumigation. The start of the latter step coincides with peak accumulation of $H_2O_2$ (Figures 1 and 2). The results suggested that the effects of $ClO_2$ fumigation on altering Prx and Trx redox state may be done over $H_2O_2$ signaling.

Prx, Trx and TrxR work in concert neutralizing harmful $H_2O_2$. The enzyme Prx of the Prx-Trx system itself is the target of $H_2O_2$ signaling (Randall et al., 2013). Upon reacting with $H_2O_2$, Prx becomes oxidized. Recycling oxidized Prx also renders Trx oxidized (Brown et al., 2013; Netto and Antunes, 2016). If the activity of these enzymes intensifies, $Prx_{ox}/Prx_{red}$ and $Trx_{ox}/Trx_{red}$ ratios would definitely elevate. The results clearly support this notion. During the first 6 h after fumigation, both Prx and Trx activity were induced (Figure 3) matching with abrupt increase in $H_2O_2$ (Figure 1). Accumulation of oxidized state of Prx and Trx induced by $H_2O_2$ was also found in barley (König et al., 2002), Chinese cabbage (Kim et al., 2009) and yeast (Bozonet et al., 2005; Brown et al., 2013). Hence, it is plausible that one of the targets of $H_2O_2$ signaling induced by $ClO_2$ is Prx in the Prx-Trx system. It is interesting to note that at 24 h after fumigation, $Prx_{ox}/Prx_{red}$ and $Trx_{ox}/Trx_{red}$ ratios abruptly dropped (Figure 2) while Prx and TrxR activities decreased slowly over the rest of the storage period. This could be due to other factor, possibly cellular NADPH redox equilibrium.

$ClO_2$ fumigation altered NADPH redox equilibrium of longan pericarp to a higher NADPH/NADP ratio and lower NADPH redox potential (Figure 5). This might result in a stable NADPH redox state for various biochemical reactions, including the Prx-Trx system and the antioxidant defense system (Valderrama et al., 2006; Meyer et al., 2008). It is possible that $ClO_2$ enhances NADPH-regenerating enzymes such as glucose-6-phosphate dehydrogenase and 6-phosphogluconate dehydrogenase (Chumyam et al., 2017). The higher NADPH/NADP ratio and lower NADPH redox potential induced by $ClO_2$ may be exploited more effectively in upregulation of Prx-Trx cycling by turning oxidized Prx and Trx to their reduced forms and increasing Prx and TrxR activities to scavenge $H_2O_2$ efficiently (Figures 3 and 5). The activation of this redox cycling led to the reduction of $H_2O_2$ signal level and oxidation state of Trx and Prx after 24 h of storage (Figures 1 and 2). The results are in line with the work of Chumyam et al. (2019) who found that higher NADPH/NADP ratio enhanced the Prx-Trx cycling.

MAPK cascades are activated upon perception of several stimuli affecting cellular events including stress response. In this study, $ClO_2$ induced the accumulation of MPK3 and MPK6 in longan pericarp. The kinases buildup started immediately upon fumigation, peaked at 12 h and persisted up to 120 h (Figure 4). The peak accumulation followed the peak increase of $H_2O_2$ (Figure 1) suggesting the signaling event utilizes the MAPK cascade. $H_2O_2$ has been shown to induce AtMPK3 and AtMPK6 activation in *Arabidopsis* (Liu and He, 2017) and MAPKs in maize (Ding et al., 2009; Zong et al., 2009), in pea (Ortiz-Masia et al., 2008) and in rice (Prasad et al., 1994; Xie et al., 2009). Three activation pathways have been proposed; direct activation of the kinases, indirect activation through ROS homeostasis and inactivation of MAPK repressors (Brown et al., 2013; Netto and Antunes, 2016 and Liu and He, 2017).

$ClO_2$ treatment has been demonstrated to delay pericarp browning in longan fruit by upregulating gene expression of the antioxidant defense-related enzymes such as superoxide dismutase, catalase and ascorbate peroxidase in harvested longan during storage at room temperature (Chomkitichai, 2014). This upregulation may be a result of activation through MPK3 and MPK6 by $H_2O_2$ signaling (Muhammad et al., 2019). In addition, the $H_2O_2$ signaling also affects Prx-Trx system causing an increase in the NADPH/NADP ratio. The ascorbate-glutathione cycle is, in turn, positively regulated inducing tolerance to oxidative stress (Chumyam et al., 2017).

From this study, a possible model by which $ClO_2$ modulates the redox state of Prx and Trx in $H_2O_2$ sensing and MAPK accumulation is proposed (Figure 8). $ClO_2$ induces transient $H_2O_2$ production and modulates Prx-Trx redox system by controlling NADPH redox potential. The induced $H_2O_2$ signaling and altered Prx and Trx redox state at early

storage period promote MPK3 and MPK6 accumulation stimulating antioxidant defense system. Oxidative damage from ROS such as $H_2O_2$ and pericarp browning of longan fruit during storage are, therefore, reduced.
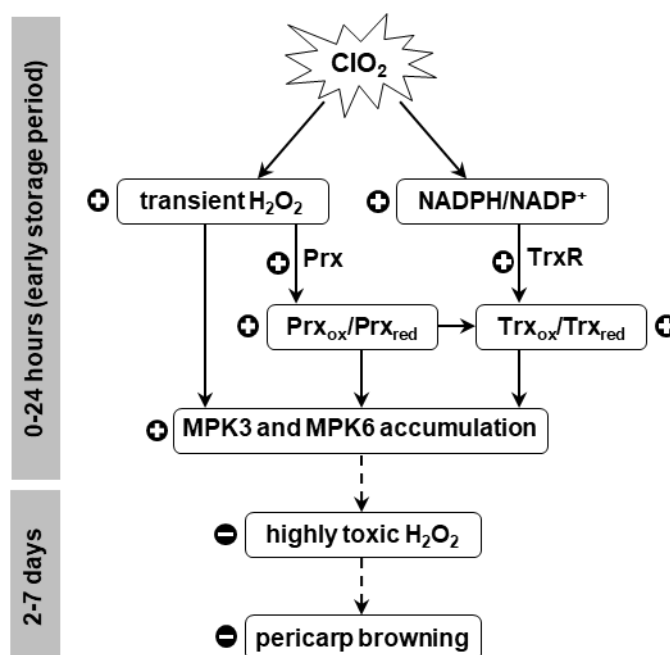


**Figure 8.** **Proposed mechanism for longan pericarp browning reduction by ClO$_2$ via activating signal transduction through Prx-Trx system during storage (+ = activation effect, - = inhibitory effect).**

## CONCLUSION

The present study demonstrates that ClO$_2$-induced transient $H_2O_2$ accumulation triggered the accumulation of MAPKs through the alteration of Prx and Trx redox state in $H_2O_2$ sensing. The accumulation of this signal transduction subsequently enhanced antioxidant defense system to remove toxic $H_2O_2$ and other ROS. These effects led to the reduction in pericarp browning of harvested longan fruit. Further studies are needed to evaluate another signaling pathway involved in pericarp browning of longan fruit.

## REFERENCES

Arnér, E.S.J., Zhong, L., and Holmgren, A. 1999. Preparation and assay of mammalian thioredoxin and thioredoxin reductase. Methods Enzymology. 300: 226-239.

Bozonet, S.M., Findlay, V.J., Day, A.M., Cameron, J., Veal, E.A., and Morgan, B.A. 2005. Oxidation of a eukaryotic 2-Cys peroxiredoxin is a molecular switch controlling the transcriptional response to increasing levels of hydrogen peroxide. The Journal of Biological Chemistry. 280: 23319-23327.

Brown, J.D., Day, A.M., Taylor, S.R., Tomalin, L.E., Morgan, B.A., and Veal, E.A. 2013. A peroxiredoxin promotes $H_2O_2$ signaling and oxidative stress resistance by oxidizing a thioredoxin family protein. Cell Reports. 5: 1425-1435.

Brugidou, C., Rocher, A., Giraud, E., Lelong, B., Marin, B., and Raimbault, M. 1991. A new high performance liquid chromatographic technique for separation and determination of adenylic and nicotinamide nucleotides in *Lactobacillus plantarum*. Biotechnology Techniques. 5: 475-578.

Chomkitichai, W. 2014. Effects of gaseous chlorine dioxide fumigation on oxidative damage and antioxidant defense system involved in pericarp browning during storage of longan fruit cv. Daw [dissertation]. Chiang Mai: Chiang Mai University.

Chomkitichai, W., Chumyam, A., Rachtanapun, P., Uthaibutra, J., and Saengnil, K. 2014a. Reduction of reactive oxygen species production and membrane damage during storage of 'Daw' longan fruit by chlorine dioxide. Scientia Horticulturae. 170: 143-149.

Chomkitichai, W., Faiyue, B., Rachtanapun, P., Uthaibutra, J., and Saengnil, K. 2014b. Enhancement of the antioxidant defense system of post-harvested 'Daw' longan fruit by chlorine dioxide fumigation. Scientia Horticulturae. 178: 138-144.

Chumyam, A., Faiyue, B., and Saengnil, K. 2019. Reduction of enzymatic browning of fresh-cut guava fruit by exogenous hydrogen peroxide-activated peroxiredoxin/thioredoxin system. Scientia Horticulturae. 255: 260-268.

Chumyam, A., Shank, L., Faiyue, B., Uthaibutra, J., and Saengnil, K. 2017. Effects of chlorine dioxide fumigation on redox balancing potential of antioxidative ascorbate-glutathione cycle in 'Daw' longan fruit during storage. Scientia Horticulturae. 222: 76-83.

Cross, J.V., and Templeton, D.J. 2006. Regulation of signal transduction through protein cysteine oxidation. Antioxidants and Redox Signaling. 8: 1819-1827.

Dai, H., Jia, G., and Shan, C. 2015. Jasmonic acid-induced hydrogen peroxide activates MEK1/2 in upregulating the redox states of ascorbate and glutathione in wheat leaves. Acta Physiologiae Plantarum. 37: 200.

Dat, J.F., Lopez-Delgado, H., Foyer, C.H., and Scott, I.M. 1998. Parallel changes in $H_2O_2$ and catalase during thermotolerance induced by salicylic acid or heat acclimation in mustard seedlings. Plant Physiology. 116: 1351-1357.

Dietz, K., Jacob, S., Oelze, M., Laxa, M., Tognetti, V., Marina, S., Miranda, N., Baier, M., and Finkemeier, I. 2006. The function of peroxiredoxins in plant organelle redox metabolism. Journal of Experimental Botany. 57: 1697-1709.

Ding, H.D., Zhang, X.H., Xu, S.C., Sun, L.L., Jiang, M.Y., Zhang, A.Y., and Jin, Y.G. 2009. Induction of protection against paraquat-induced oxidative damage by abscisic acid in maize leaves is mediated through mitogen-activated protein kinase. Journal of Integrative Plant Biology. 51: 961-972.

Frey, N.F., Garcia, A.V., Bigeard, J., Zaag, R., Bueso, E., Garmier, M., Pateyron, S., Tauzia-Moreau, M., Brunaud, V., Balzergue, S., Colcombet, J., Aubourg, S., Martin-Magniette, M., and Hirt, H. 2014. Functional analysis of Arabidopsis immune-related MAPKs uncovers a role for MPK3 as negative regulator of inducible defences. Genome Biology. 15: R87.

Go, Y.M., and Jones, D.P. 2009. Thioredoxin redox western analysis. Current Protocols in Toxicology. 41: 17.12.1-17.12.12.

Jiang, Y.M., and Li, Y.B. 2001. Effects of chitosan coating on postharvest life and quality of longan fruit. Food Chemistry. 73: 139-143.

Joradol, A., Uthaibutra, J., Lithanatudom, P., and Saengnil, K. 2019. Induced expression of NOX and SOD by gaseous sulfur dioxide and chlorine dioxide enhances antioxidant capacity and maintains fruit quality of 'Daw' longan fruit during storage through $H_2O_2$ signaling. Postharvest Biology and Technology. 156: 110938.

Kim, S.Y., Jang, H.H., Lee, J.R., Sung, N.R., Lee, H.B., Lee, D.H., Park, D.J., Kang, C.H., Chung, W.S., Lim, C.O., et al. 2009. Oligomerization and chaperone activity of a plant 2-Cys peroxiredoxin in response to oxidative stress. Plant Science. 177: 227-232.

Kovtun, Y., Chiu, W.L., Tena, G., and Sheen, J. 2000. Functional analysis of oxidative stress activated mitogen-activated protein kinase cascade in plants. Proceedings of the National Academy of Sciences of the United States of America. 97: 2940-2945.

König, J., Baier, M., Horling, F., Kahmann, U., Harris, G., Schürmann, P., and Dietz, K. 2002. The plant-specific function of 2-Cys peroxiredoxin mediated detoxification of peroxides in the redox-hierarchy of photosynthetic electron flux. Proceedings of the National Academy of Sciences of the United States of America. 99: 5738-5743.

Liu, Y., and He, C. 2017. A review of redox signaling and the control of MAP kinase pathway in plants. Redox Biology. 11: 192-204.

Lowry, O.H., Rosebrough, N.J., Far, A.L., and Randall, R.J. 1951. Protein measurement with the folin phenol reagent. Journal of Biological Chemistry. 193: 265-275.

Meyer, Y., Siala, W., Bashandy, T., Riondet, C., Vignols, F., and Reichheld, J.P. 2008. Glutaredoxins and thioredoxins in plants. Biochimica et Biophysica Acta. 1783: 589-600.

Muhammad, T., Zhang, J., Ma, Y., Li, Y., Zhang, F., Zhang,Y., and Liang, Y. 2019. Overexpression of a mitogen-activated protein kinase *SlMAPK3* positively regulates tomato tolerance to cadmium and drought stress. Molecules. 24: 556.

Muniyappa, H., Song, S., Mathews, C.K., and Das, K.C. 2009. Reactive oxygen species-independent oxidation of thioredoxin in hypoxia: inactivation of ribonucleotide reductase and redox-mediated checkpoint control. Journal of Biological Chemistry. 284: 17069-17081.

Netto, L.E., and Antunes, F. 2016. The roles of peroxiredoxin and thioredoxin in hydrogen peroxide sensing and in signal transduction. Molecules and Cells. 39: 65-71.

Ortiz-Masia, D., Perez-Amador, M.A., Carbonell, P., Aniento, F., Carbonell, J., and Marcote, M.J., 2008. Characterization of PsMPK2, the first C1 subgroup MAP kinase from pea (*Pisum sativum* L.). Planta. 227: 1333-1342.

Pannala, V.R., and Dash, R.K. 2015. Mechanistic characterization of the thioredoxin system in the removal of hydrogen peroxide. Free Radical Biology and Medicine. 78: 42-55.

Pascual, M.B., Mata-Cabana, A., Florencio, F.J., Lindahl, M., and Cejudo, F.J. 2011. A comparative analysis of the NADPH thioredoxin reductase C-2-Cys peroxiredoxin system from plants and cyanobacteria. Plant Physiology. 155: 1806-1816.

Prasad, T.K., Anderson, M.D., Martin, B.A., and Stewart, C.R. 1994. Evidence for chilling-induced oxidative stress in maize seedlings and a regulatory role for hydrogen peroxide. Plant Cell. 6: 65-74.

Randall, L.M., Ferrer-Sueta, G., and Denicola, A. 2013. Chapter Three - Peroxiredoxins as preferential targets in $H_2O_2$-induced signaling. Methods in Enzymology. 527: 41-63.

Rhee, S.G., Chang, T.S., Bae, Y.S., Lee, S.R., and Kang, S.W. 2003. Cellular regulation by hydrogen peroxide. Journals of the American Society of Nephrology. 14: S211-S215.

Rhee, S.G., Woo, H.A., Kil, I.S., and Bae, S.H. 2012. Peroxiredoxin functions as a peroxidase and a regulator and sensor of local peroxides. Journal of Biological Chemistry. 287: 4403-4410.

Saengnil, K., Chumyam, A., Faiyue, B., and Uthaibutra, J. 2014. Use of chlorine dioxide fumigation to alleviate enzymatic browning of harvested 'Daw' longan pericarp during storage under ambient conditions. Postharvest Biology and Technology. 91: 49-56.

Schafer, F.Q., and Buettner, G.R. 2001. Redox environment of the cell as viewed through the redox state of the glutathione disulfide/glutathione couple. Free Radical Biology and Medicine. 30: 1191-1212.

Sevilla, F., Camejo, D., Ortiz-Espín, A., Calderón, A., Lázaro, J.J., and Jiménez, A. 2015. The thioredoxin/peroxiredoxin/sulfiredoxin system: current overview on its redox function in plants and regulation by reactive oxygen and nitrogen species. Journal of Experimental Botany. 66: 2945-2955.

Sharma, P., Jha, A.B., Dubey, R.S., and Pessarakli, M. 2012. Reactive oxygen species, oxidative damage, and antioxidative defense mechanism in plants under stressful conditions. Journal of Botany. 2012: 1-26.

Ślesak, I., Libik, M., Karpinska, B., Karpinski, S., and Miszalski, Z. 2007. The role of hydrogen peroxide in regulation of plant metabolism and cellular signalling in response to environmental stresses. Acta Biochimica Polonica. 54: 39-50.

Supapvanich, S., Pimsaga, J., and Srisujan, P. 2011. Physiochemical changes in fresh-cut wax apple (*Syzygium samarangenese* Blume Merrill & L.M. Perry) during storage. Food Chemistry. 127: 912-917.

Valderrama, R., Corpas, F.J., Carreras, A., Gómez-Rodríguez, M.V., Chaki, M., Pedrajas, J.R., Fernández-Ocaña, A., Del Río, L.A., and Barroso, J.B. 2006. The dehydrogenase-mediated recycling of NADPH is a key antioxidant system against salt-induced oxidative stress in olive plants. Plant Cell and Environment. 29: 1449-1459.

Veal, E.A., Day, A.M., and Morgan, B.A. 2007. Hydrogen peroxide sensing and signaling. Molecules and Cells. 26: 1-14.

Velikova, V., Yordanov, I., and Edreva, A. 2000. Oxidation stress and some antioxidant systems in acid rain-treated bean plant: protective role of exogenous polyamines. Plant Science. 151: 59-66.

Xie, G., Kato, H., Sasaki, K., and Imai, R. 2009. A cold-induced thioredoxin h of rice, OsTrx23, negatively regulates kinase activities of OsMPK3 and OsMPK6 in vitro. Federation of European Biochemical Societies Letters. 583: 2734-2738.

Ye, L., Li, L., Wang, L., Wang, S., Li, S., Du, J., Zhang, S., and Shou, H. 2015. MPK3/MPK6 are involved in iron deficiency-induced ethylene production in Arabidopsis. Frontiers in Plant Science. 6: 953.

Zhu, F., Chen, J., Xiao, X., Zhang, M., Yun, Z., Zeng, Y., Xu, J., Cheng, Y., and Deng, X. 2016. Salicylic acid treatment reduces the rot of postharvest citrus fruit by inducing the accumulation of $H_2O_2$, primary metabolites and lipophilic polymethoxylated flavones. Food Chemistry. 207: 68-74.

Zong, X.J., Li, D.P., Gu, L.K., Li, D.Q., Liu, L.X., and Hu, X.L. 2009. Abscisic acid and hydrogen peroxide induce a novel maize group C MAP kinase gene, ZmMPK7, which is responsible for the removal of reactive oxygen species. Planta. 229: 485-495.